Luminescence dating report

Project: Steinke-Ward

Forget Brisson, L., Hardy, F. and Lamothe, M.
Laboratoire LUX, Université du Québec à Montréal

Content

Mandate

Four samples were submitted to the LUX luminescence dating laboratory of UQAM in 2022 by Jessi Steinke and Professor Brent Ward, both associated with the Earth Science Department of the Simon Fraser University. Samples were collected near the hamlet of Keno City (Keno Hill), on the Na-Cho Nyak Dun land, in the Central-Yukon area, Canada (Fig. 1). This zone is bordered to the north by the Mackenzie Mountains and to the south by the Stewart River valley.

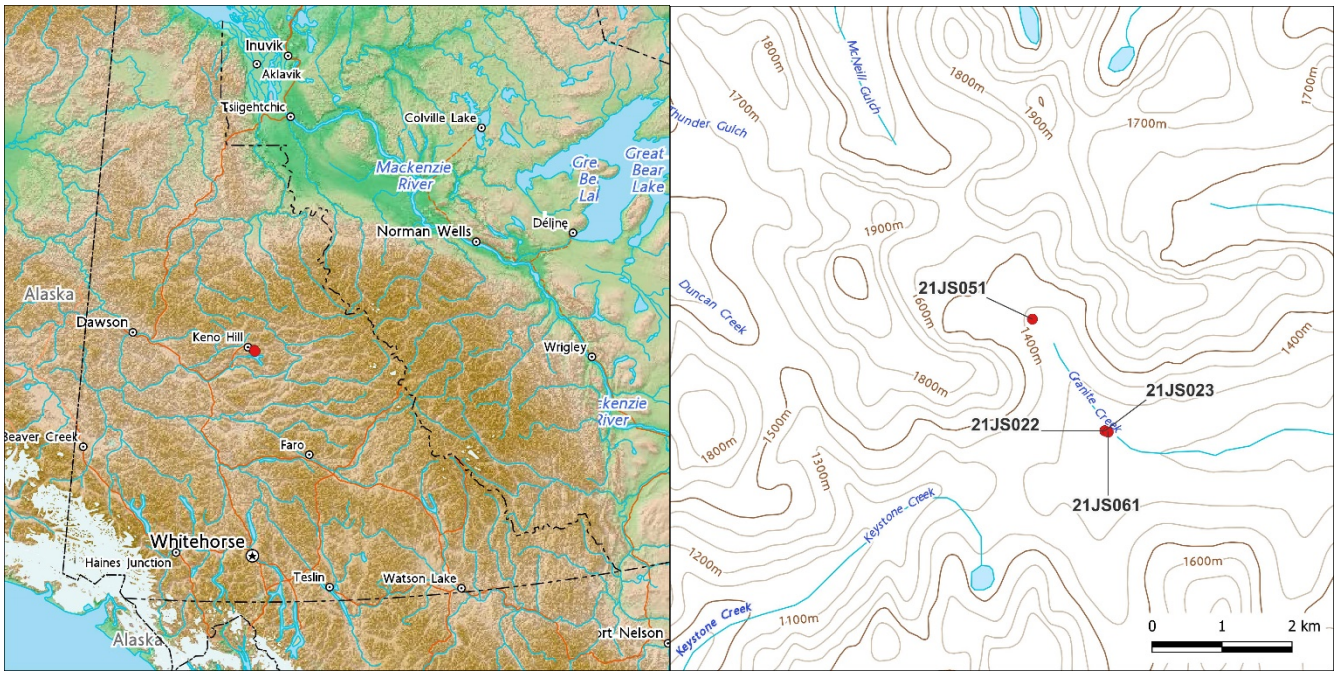

Figure 1: Samples location maps in Yukon, Canada.

According to the provided sampling report (annexe), the two first samples, 21JS-022 and 21JS-023, are from unit 8 of the GRC-01W section. This unit is described as a thin (0.25 to 1.25 m) discontinuous, oxidized, mottled and crudely bedded silty sand interpreted to be MIS 4/3 in age. Since there is a major disturbance visible on the picture given for sample 21JS-023, sample 21JS-022 is preferred to date this unit, from a luminescence point of view.

Sample 21JS-051, collected from section GRC-05U, is from a layer previously though to be unit 8 (MIS 4/3), but could also be younger (unit 14?). This unit is described as a very thin layer (0.2 to 0.5 m) of oxidized clayey silt with pebbles. According to the picture, the silt layer is very thin and within much coarser material including blocks. As for sample 21JS-023, this situation could lead to a serious disparity between the measured annual dose rate (D_a) and the *in situ* condition, causing an error in age determination.

Lastly, sample 21JS-061 is from unit 3 of the GRC-01S section (or GRC-01W?). This unit is interpreted to be a MIS 6 or MIS 4 glaciofluvial sand lens of 0 to 3 m in thickness, which is glaciotectonized and incorporated into a till layer. Concerns must be expressed about the position of the luminescence sample near the border of the lens. This could again significantly complicate the annual dose rate determination.

Samples were submitted to determine the age of their deposition and to validate unit association across the different sections. However, the potential precision of the dating results is hindered by the less-than-ideal sampling situation of samples 21JS-023, 21JS-051 and 21JS-061. Ideal sampling conditions can be visualized in Fig. 2. The collected samples for luminescence dating hence should be at a minimum of 30 cm away from any disturbance or heterogeneity.

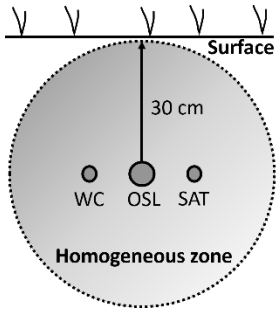

Figure 2: Schematic ideal sampling conditions. In this example, 3 tubes are collected near each other: "OSL" for luminescence dating measurements, "WC" and "SAT" for water content and water saturation determination, respectively. Sediments from a 30 cm radius from the OSL tube can also be collected in a sample bag for D_a evaluation.

Principles and methodology

The luminescence dating method exploits a property of certain minerals, such as quartz and feldspar, that is the emission of photons when they are optically stimulated (Optically Stimulated Luminescence; OSL) or thermally stimulated (Thermoluminescence; TL). The intensity of the emitted luminescence signal is proportional to the radioactive dose received during burial, which is considered to be constant over time. Minerals in the sediment hence act as dosimeters for the natural radioactivity in the environment by trapping, in their crystalline structure, electrons excited by the ionizing energy coming from the radioactive decay of certain natural radioactive isotopes. Uranium (U), thorium (Th) and potassium (K) are the main radioisotopes contributing to environmental radioactivity, to which is added a contribution from cosmic radiation.

By monitoring the natural luminescence signal, as well as the signal induced by artificial radioactive doses (thus delivering the equivalent dose – D_e) and by estimating the amount of radiation received annually by the sample while buried in the ground (annual dose – D_a), it is possible to determine the amount of time elapsed since burial, considered here as the age of the sediments (Rodhes 2011; Duller 2008; Aitken 1985, 1998). This can be expressed by this equation:

$$Age\ (ka) = \frac{D_e\ (Gy)}{D_a\ (Gy/ka)}$$ [1]

Sample preparation

The tubes used for sediment sampling were opened in the LUX laboratory under controlled lighting. The sediment portion at the extremities of the tubes were removed and used for D_a assessment. These sediments were dried, crushed, homogenized and settled into a paraffin puck to prevent any gas loss. Samples were then measured using a high-resolution gamma spectrometer for the determination of U, Th and K abundances for a duration of 72 h, a minimum of 21 days after the preparation of the puck to assure the restoration of the balance in the uranium decay chain.

Sediments in the inner portion of the tubes were used for D_e measurements. These were sieved to isolate the fraction between 64 and 90 µm. The samples were treated using HCl (20%) and H_2O_2 (30%) to remove carbonates

[1] Where ka corresponds to *kiloannum* (1000 years) and Gray (Gy) is the SI (International system) unit of radiation absorption and corresponds to 1 $J{\cdot}kg^{-1}$.

and organic matter. Samples were not mineralogically separated. Grains were disposed on stainless steel cups, covering a 2 mm diameter surface.

In situ water content (WC) was measured on the sediment portion collected at the extremities of the OSL tubes before the preparation of the paraffin puck. WC was also measured on the sediment collected in the WC tubes, before assessing the maximum water content that the sediment could hold (saturation; SAT).

For WC determination, the weight of the samples characterized by the *in situ* humidity was compared to the weight of the same sample which has been dried. In the case of SAT determination, the difference considered was between the weight of the water-saturated and the dried sediments. WC values used for D_a calculation were selected based on WC and SAT results, as well as geological contexts and speculation over the WC evolution through time. The results are presented in Table 1.

Table 1 : Water content results.

Sample	Water content (%)			
	Ext OSL tubes	WC tubes	Max (SAT)	Selected value
21JS-022	16	35	25	15 ± 5
21JS-023	12			15 ± 5
21JS-051	44	30	48	30 ± 10
21JS-061	9	8	14	8 ± 5

Measurements

Equipment

U, Th and K concentrations were measured using a high-resolution gamma spectrometer. Luminescence measurements were performed on a Lexsyg Research reader equipped with an internal beta source ($\dot{D}\beta(^{90}Sr)$ = ~0.057 Gy/s). Heating procedures were carried out in a helium atmosphere, to enhance thermal conductivity (Huot 2007). IR diodes provided a 150 mW/cm^2 stimulation at 850 ± 20 nm. The detection window was centered at 410 nm, with the combination of Schott-BG 39 (3 mm) and AHF-BrighLine HC 414/46-Interference (3.5 mm) filters.

Annual dose rate (D_a)

U, Th and K concentration, as well as location parameters (*i.e.* altitude, latitude, longitude and depth from the surface), and water content were used for sample's D_a determination. D_a were calculated using the DRAC (Dose Rate and Age Calculator; Durcan et al. 2015). Conversion factors from Adamiec and Aitken (1998) were used, as for alpha and beta attenuation factor from Bell (1980) and Mejdahl (1979), respectively. The selected *a*-value was 0.10 ± 0.02 (Balescu and Lamothe 1994). Internal K content was set to 10 ± 2 % (Smedley et al. 2012). The selected water content for each sample is shown in Table 1.

Equivalent dose (D_e)

D_e were measured following a SAR protocol (*Single Aliquot Regeneration dose* - Murray and Wintle, 2000; Lamothe 2004), the $pIR_{50}IR_{225}$ (Thomsen et al. 2008; Lamothe et al. 2018). This methodology involves the measurement of the luminescence signal from two consecutive IR stimulation performed at different temperatures (at 50 and 225°C, in this case). For each temperature, the normalized natural luminescence signal of an aliquot is projected on a growth curve constructed using the normalized luminescence response to beta doses of various sizes of the

same aliquot. The *global standardized growth curve* methodology (gSGC; Li *et al.* 2015) was used to reduce measurement time. Following this procedure, for each step, the sum of the luminescence signal from 3 aliquots was used to produce a "synthetic aliquot", which is considered to act as a representative aliquot for each sample. A standardized and universal growth curve was thus produced for each sample, on which the natural luminescence measurements (Ln/Tn) of 12 aliquots were reported and normalized. The constructed growth curves for IR50 and IR225 can be visualized in Fig. 3, while the protocol used is presented in Table 2. For each temperature, the luminescence signal is assessed by subtracting the integral of the last 20 s of the IRSL decay curves (corresponding to the background) from the initial signals, which correspond to the first 5 s of the decay curve.

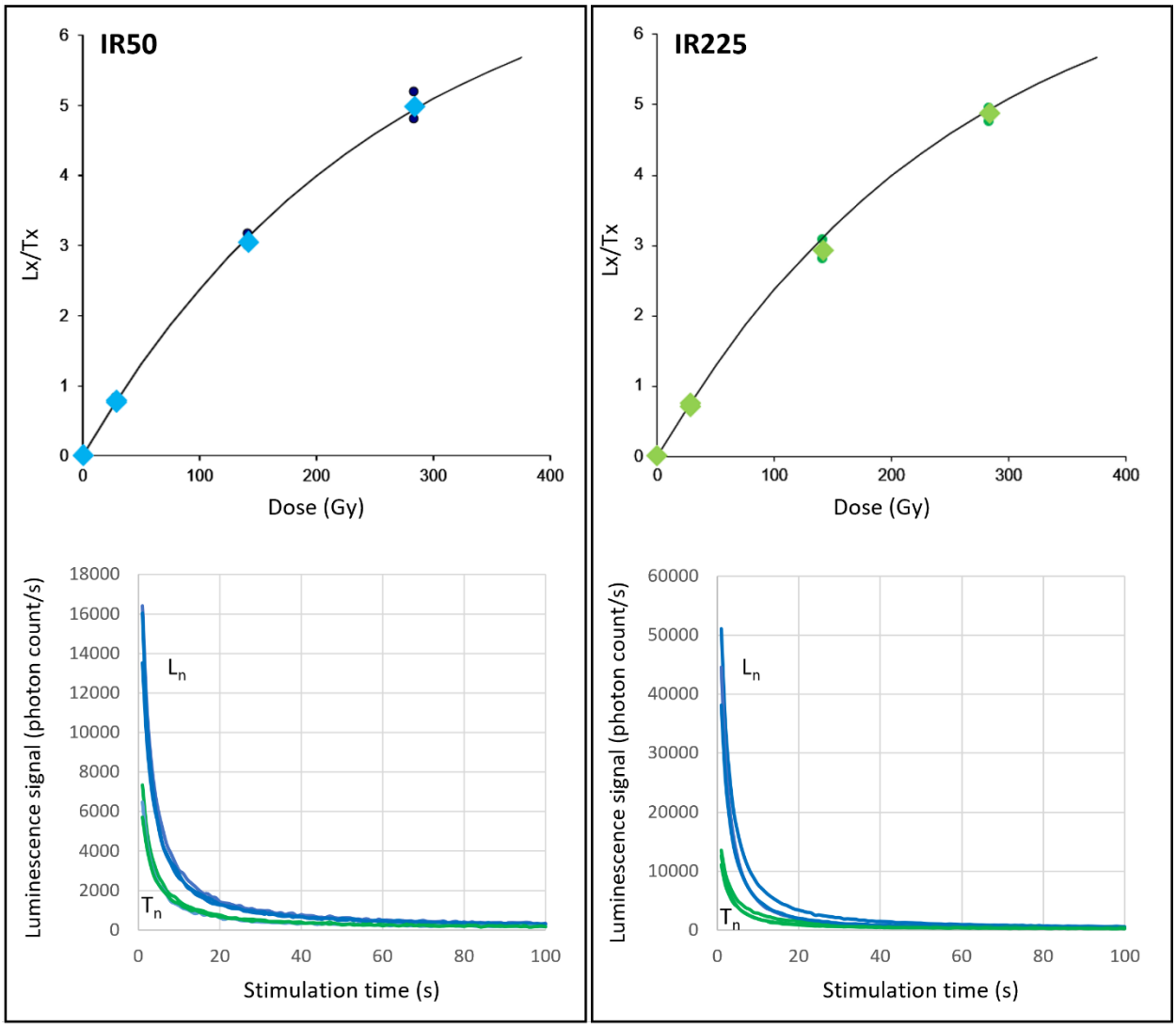

Figure 3 : Top. IR50 and IR225 growth curves of the sample 21JS-022. The normalized luminescence signals of the three measured aliquots are shown (dark dot) as well as the "synthetic aliquots" (sum of the signal; light colored diamond). Error bars are hidden by the symbols. Bottom. IR50 and IR225 decay curves for the natural luminescence signal (Ln; blue) and the natural test dose (Tn; green) for the three aliquots used to construct the growth curves.

Table 2 : $pIR_{50}IR_{225}$ protocol

Step			Details
Dose – Ln and Lx	1	Irradiation	0 Gy for natural; ~28 Gy; ~142 Gy; ~283 Gy; 0 Gy; ~28 Gy
	2	Preheat	250°C, 60 s
	3	IRSL	50°C, 100 s
	4	IRSL	225°C, 100 s
Test dose – Tn and Tx	5	Irradiation	~34 Gy
	6	Preheat	250°C, 60 s
	7	IRSL	50°C, 100 s
	8	IRSL	225°C, 100 s
	9	IRSL	325°C, 100 s
Return to step 1			

g values

Feldspars are affected by an abnormal decrease in their luminescent signal and this phenomenon is known as anomalous fading (Aitken 1985, 1998; Huntley and Lamothe 2001; Lamothe et al. 2003). Trapped electrons, instead of remaining in the crystal traps, escape through tunnel effect. This phenomenon leads to an overestimation of the regenerated luminescent signal, and therefore to an underestimation of the age of the sample. D_e must be corrected according to the anomalous fading rate of the samples (*g* value) to obtain adequate age results. *g* values were measured on six aliquots by sample following a protocol similar to the one presented in Table 2, but by inserting delay of various length between steps 2 and 3 (Auclair et al. 2003).

Results

D_a

D_a were obtained for each sample and results are indicated in Table 3.

Table 3 : Abundances and D_a results

Sample	Abundance			External dose rate (Gy/ka)				Internal dose rate (Gy/ka)	D_a (Gy/ka)
	U (ppm)	Th (ppm)	K (%)	Alpha	Beta	Gamma	Cosmic	Beta	
21JS-022	4.32 ± 0.11	10.59 ± 0.21	1.41 ± 0.04	0.49 ± 0.10	1.61 ± 0.09	1.14 ± 0.06	0.08 ± 0.01	0.27 ± 0.06	3.60 ± 0.16
21JS-023	3.95 ± 0.09	9.79 ± 0.19	1.39 ± 0.03	0.45 ± 0.09	1.54 ± 0.09	1.07 ± 0.05	0.08 ± 0.01	0.27 ± 0.06	3.42 ± 0.15
21JS-051	4.55 ± 0.11	11.73 ± 0.23	1.44 ± 0.04	0.45 ± 0.10	1.45 ± 0.14	1.06 ± 0.09	0.14 ± 0.01	0.27 ± 0.06	3.38 ± 0.20
21JS-061	2.14 ± 0.06	5.09 ± 0.12	0.57 ± 0.02	0.26 ± 0.05	0.77 ± 0.05	0.57 ± 0.03	0.04 ± 0.01	0.27 ± 0.06	1.92 ± 0.10

D_e and *g* values

Dose recovery test

Dose recovery tests (DRT; Wallinga *et al.* 2000) were performed on two samples (21JS-022 and 21JS-051) in order to test and validate the selected measurement protocol for D_e determination. In this procedure, the natural signal of three aliquots per sample is removed by light exposure (Honle SOL2 sun simulator for 1 h) and a known radiation dose is given in the lab (*i.e.* ~85 Gy). The protocol presented in Table 2 is then performed and the obtained D_e is compared to the given dose, corresponding to the dose recovery ratio (DRR). DRR should fall between the acceptable range of 0.90 to 1.10 for a protocol to be considered as successful. Obtained DRR are presented in

Fig. 4 for each stimulation temperatures (IR50 and IR225). For both samples, the average values (Central Age Model – CAM; Galbraith *et al.* 1999) of the IR50 signal is contained in the acceptable range (0.93 ± 0.02 for 21JS-022 and 0.94 ± 0.03 for 21JS-051). However, in the case of the IR225 signal, the averaged DRR is above the limit for 21JS-022 (1.22 ± 0.04), while the value for 21JS-051 is at the limit of the acceptable range (1.10 ± 0.02).

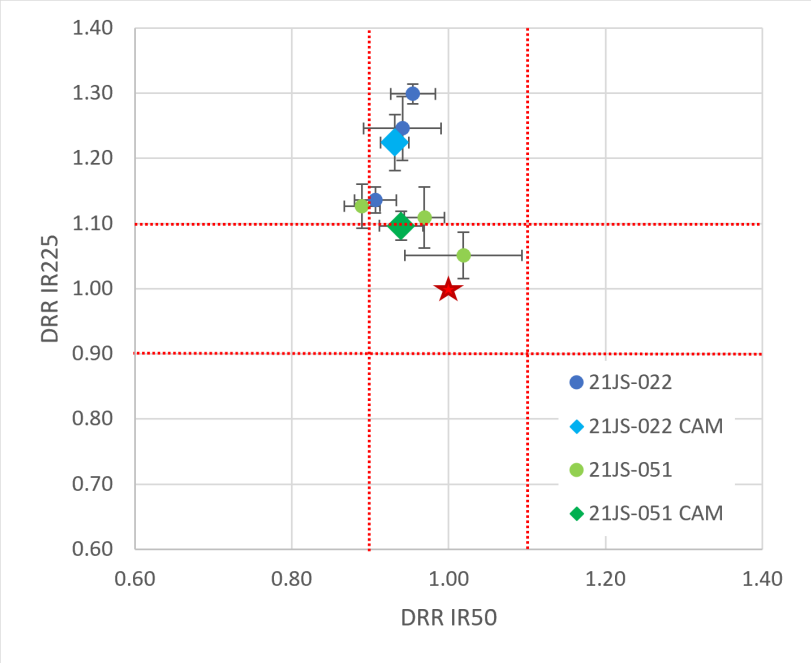

Figure 4 : Individual (dots) and average (diamond) DRR (IR50 in x and IR225 in y) for 21JS-022 (blue) and 21JS-051 (green). The acceptable range are indicated for both axis by red dotted lines. The optimal value (IR50=IR225=1.00) is indicated by a red star.

D_e distributions

Distributions for the uncorrected D_e (IR50 and IR225) are shown in Fig. 5 to 8 for samples 21JS-022, 21JS-023, 21JS-051 and 21JS-061, respectively.

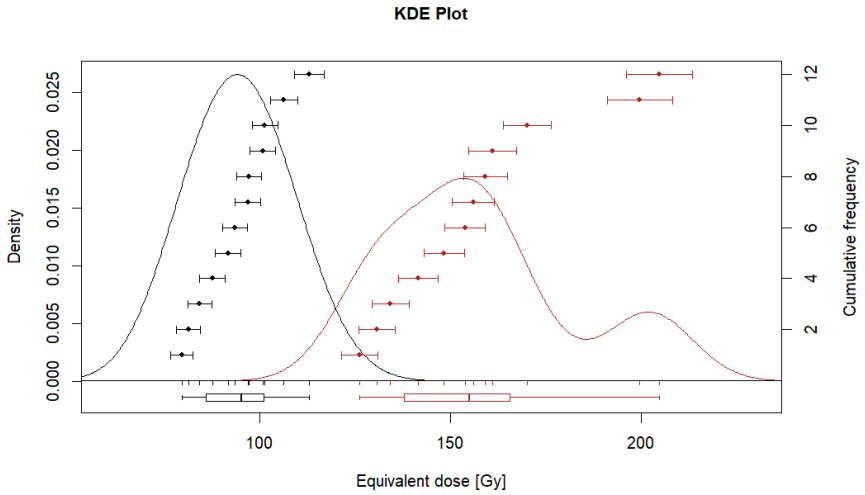

Figure 5 : De50 (black) and De225 (red) distribution for 21JS-022.

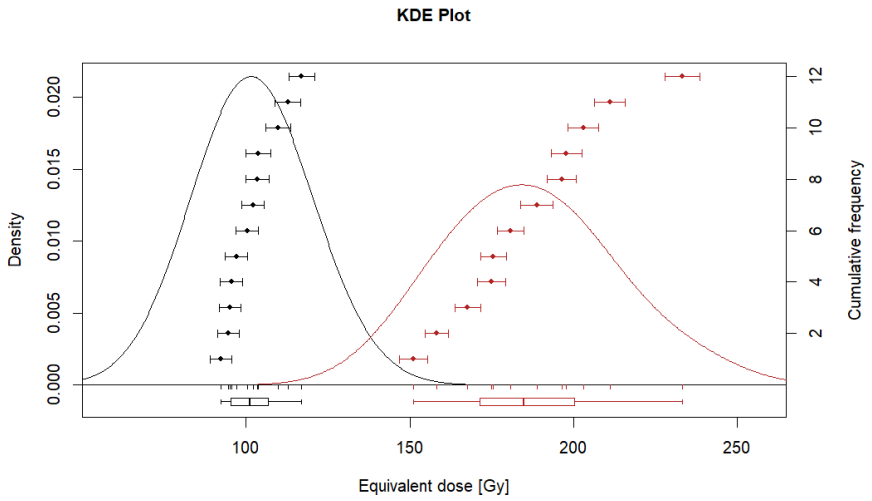

Figure 6 : De50 (black) and De225 (red) distribution for 21JS-023.

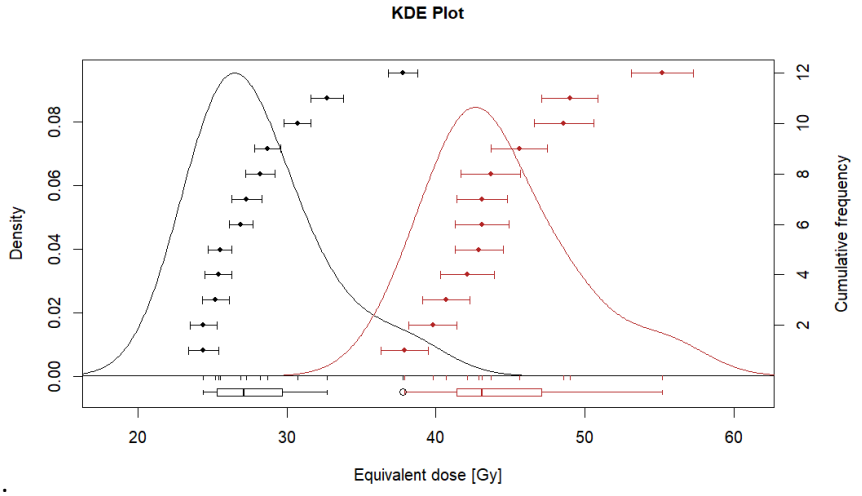

.

Figure 7 : De50 (black) and De225 (red) distribution for 21JS-051.

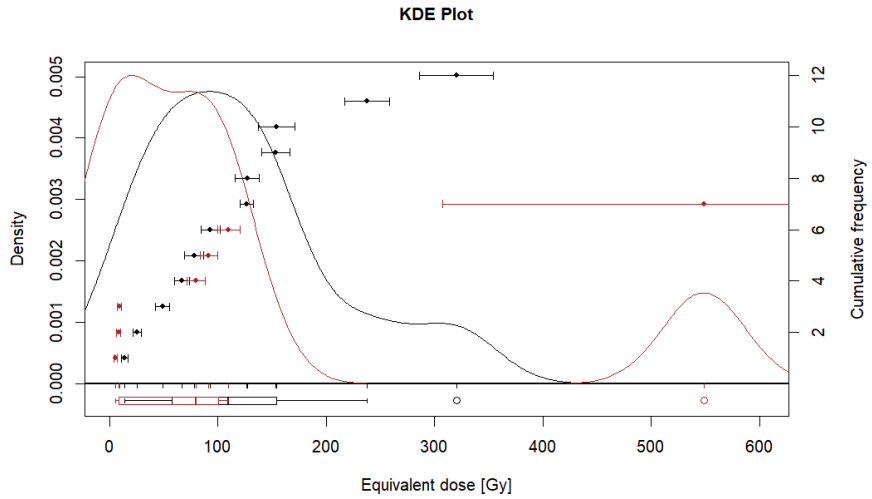

Figure 8 : De50 (black) and De225 (red) distribution for 21JS-061.

We can see that the uncorrected D_e IR50 is systematically lower than the D_e IR225 except for sample 21JS-061. Also, for the uncorrected D_e IR50, distributions are unimodal, which is expected for multi-grains aliquots due to an averaging effect. According to the *calc_AliquotSize* R script from Burrow (2022), aliquots measured in this project contain around 440 grains (2 mm diameter of grain coverage). This large number of grains on a disk can often lead to D_e overestimation as potential unbleached grains present in the sample, which emit more luminescence than bleached ones, will dominate the luminescence signal.

g values

g values obtained from the IR50 and IR225 signals of each sample are presented in Table 4 and displayed in Fig. 9 allowing to see the relationship between the 2 signals.

Table 4 : g values

Sample	g value (%/decade)	
	IR50	IR225
21JS-022	2.2 ± 0.4	1.4 ± 0.6
21JS-023	4.4 ± 0.7	2.0 ± 0.6
21JS-051	4.0 ± 0.4	1.6 ± 0.5
21JS-061	3.3 ± 0.8	0.9 ± 0.6

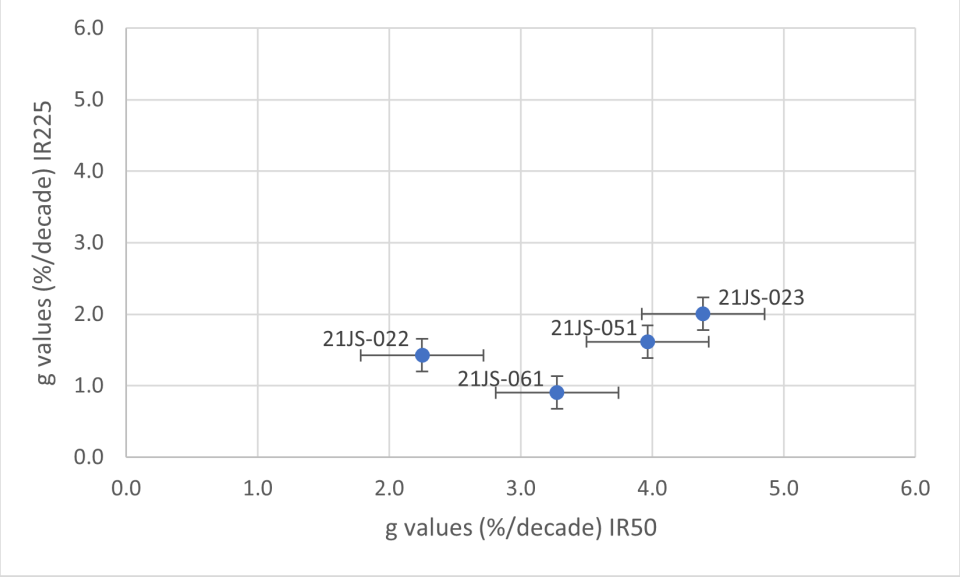

Figure 9 : Relationship between IR50 and IR225 g values for samples 21JS-022, 21JS-023, 21JS-051 and 21JS-061.

Ages

D_e were corrected for anomalous fading using the Dose rate correction (DRC; Lamothe et al. 2003). The CAM of the uncorrected and corrected are listed in Table 5 and displayed in Fig. 10 for both signals of each sample. Ages obtained using the IR50 luminescence signal are preferred here due to age overestimation that could be attributed to a residual signal affecting the higher temperature luminescence signal (IR225). Besides, DRT results suggest an inadequate use of the IR225 signal in this context.

Table 5 : Uncorrected and corrected Ages (preferred ages highlighted)

Sample	IR50		IR225	
	Age uncorr (ka)	Age corr (ka)	Age uncorr (ka)	Age corr (ka)
21JS-022	26.1 ± 1.4	32.5 ± 2.4	43.1 ± 2.6	51.1 ± 6.9
21JS-023	29.8 ± 1.4	51.3 ± 3.5	54.2 ± 3.0	71.2 ± 6.9
21JS-051	8.3 ± 0.6	12.1 ± 0.8	13.1 ± 0.8	15.2 ± 1.7
21JS-061	46.7 ± 11.7	68.0 ± 18.4	20.7 ± 12.3*	21.3 ± 12.3*

* IR225 age results (uncorrected and corrected) for the 21JS-061 sample are biased towards lower values due to 5 on 12 aliquots being in saturation.

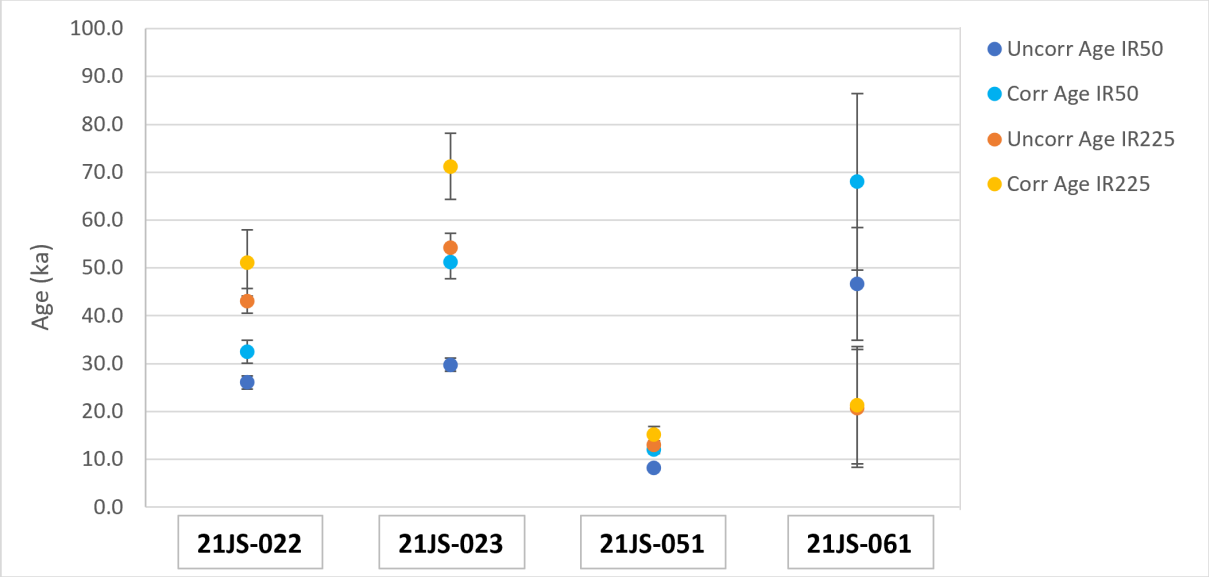

Figure 10 : Uncorrected and corrected ages for samples 21JS-022, 21JS-023, 21JS-051 and 21JS-061.

Discussion and conclusion

According to the sampling report, 21JS-022 and 21JS-023 should be from the same unit, interpreted to be MIS 4/3 in age. While these samples are not of the same age (~32.5 ka for 21JS-022 and ~51.3 ka for 21JS-023), they both fall within the MIS 3 interval. In the case of sample 21JS-051, age results (~12.1 ka) strongly indicate that the sampled layer is definitely younger than the initially hypothesized MIS 4/3 interval and should instead be associated to the late Pleistocene. The coherence between both signals (IR50 and IR225) suggests an adequate bleaching of the particles prior to deposition. Lastly, age results obtained from sample 21JS-061, despite a higher variability in individual result (see Fig. 8), allow to discard the MIS 6 hypothesis. However, sampling caveats mentioned for samples 21JS-023, 21JS-051 and 21JS-061 need to be kept in mind when interpreting the results as it could possibly limit age results validity. Hence the results are mostly indicative of a period, and not that much of an exact age.

References

Adamiec, G. et Aitken, M.J. (1998). Dose-rate conversion factors: update. Ancient TL, 16(2), 37-50.

Aitken, M. J. (1985). Thermoluminescence dating. Academic Press, London.

Aitken, M. J. (1998). An introduction to optical dating. Oxford University Press, Oxford.

Auclair, M., Lamothe, M. et Huot, S. (2003). Measurement of anomalous fading for feldspar IRSL using SAR. Radiation Measurements, 37, 487 – 492.

Balescu, S. et Lamothe, M. (1994). Comparison of TL and IRSL age estimates of feldspar coarse grains from waterlain sediments. Quaternary Science Reviews, 13, 437-444.

Bell, W.T. (1980). Alpha dose attenuation in quartz grains for thermoluminescence dating. Ancient TL, 12(4), 8.

Burow, C. (2022). calc_AliquotSize(): Estimate the amount of grains on an aliquot. Function version 0.31. In: Kreutzer, S., Burow, C., Dietze, M., Fuchs, M.C., Schmidt, C., Fischer, M., Friedrich, J., Mercier, N., Philippe, A., Riedesel, S., Autzen, M., Mittelstrass, D., Gray, H.J., Galharret, J., 2022. Luminescence: Comprehensive Luminescence Dating Data Analysis. R package version 0.9.17. https://CRAN.R-project.org/package=Luminescence.

Duller, G. A. T. (2008). Luminescence Dating : Guidelines on using luminescence dating in archaeology, English Heritage, Swindon.

Durcan, J.A., King, G.E. et Duller, G.A. (2015). DRAC: Dose Rate and Age Calculator for trapped charge dating. Quaternary Geochronology, 28, 54-61.

Galbraith, R.F., Roberts, R.G., Laslett, G.M., Yoshida, H. et Olley, J.M. (1999). Optical dating of single and multiple grains of quartz from Jinmium rock shelter, northern Australia: part I, experimental design and statistical models. Archaeometry 41, 339-364.

Huntley, D.J. et Lamothe, M. (2001). Ubiquity of anomalous fading in K-feldspars and the measurement and correction for it in optical dating. Can. J. Earth Sci. 38, 1093–1106.

Huot, S. (2007). Investigations of alternate and innovative ways of performing luminescence dating in an attempt to extend the age range. Ph.D. thesis, Aarhus Universitet.

Lamothe, M. (2004). Optical dating of pottery, burnt stones, and sediments from selected Quebec archaeological sites. Canadian Journal of Earth Sciences 41, 659-667.

Lamothe, M., Auclair, M., Hamzaoui, C. et Huot, S. (2003). Towards a prediction of long-term anomalous fading of feldspar IRSL. Radiation Measurements, 37, 4-5, 493-498.

Lamothe, M., Forget Brisson, L. et Hardy, F. (2018). Dose recovery performance in double IRSL/pIRIR SAR protocols. Radiation Measurements, 120, 120-123.

Li, B., Roberts, R.G., Jacobs, Z., Li, S.-H. and Guo, Y.J. (2015). Construction of a 'global standardised growth curve'(gSGC) for infrared stimulated luminescence dating of K-feldspar. Quaternary Geochronology, 27, 119-130.

Mejdahl, V. (1979). Thermoluminescence dating: Beta-dose attenuation in quartz grains. Archaeometry, 21(1), 61-72.

Murray, A.S. et Wintle, A.G., 2000. Luminescence dating of quartz using an improved single-aliquot regenerative-dose protocol. Radiation Measurements 32, 57-73.

Rhodes, E. J. (2011). Optically stimulated luminescence dating of sediments over the past 200,000 years . Annual Review of Earth and Planetary Sciences 39, 461-488.

Smedley, R.K., Duller, G.A.T., Pearce, N.J.G. et Roberts, H.M. (2012). Determining the K-content of single-grains of feldspar for luminescence dating. Radiation Measurements, 47(9), 790-796.

Thomsen, K.J., Murray, A.S., Jain, M. and Botter-Jensen, L. (2008). Laboratory fading rates of various luminescence signals from feldspar-rich sediment extracts. Radiation Measurements, 43, 1474-1486.

Wallinga, J., A. Murray, G. Duller, (2000). Underestimation of equivalent dose in single-aliquot optical dating of feldspars caused by preheating, Radiat. Meas., 32 (2000), pp. 691-695.

Contacts

Measurements, data analysis and report redaction were performed by Laurence Forget Brisson.
With the collaboration of François Hardy.
Supervised by Michel Lamothe.

Table 6 : Contacts

Researcher	Position	Email
Michel Lamothe	Professeur	lamothe.michel@uqam.ca
François Hardy	Agent de recherche	hardy.francois@uqam.ca
Laurence Forget Brisson	Agente de support à la recherche	forget_brisson.laurence@uqam.ca

Laboratoire de luminescence LUX - UQAM
Département des sciences de la Terre et de l'atmosphère
C.P. 8888, Succ. Centre-Ville
Montréal, QC, H3C 3P8, Canada
Tél : 514-987-3000, poste 6626
Télécopie : 514-987-7749
www.lux.uqam.ca

Annexe – Sampling report

OSL Sample Units:

Samples: All from same unit.

21-JS-022 (white tube)

21-JS-022B (Moisture)

21-JS-023 (black tube)

Unit description: Unit 8: Loess (MIS 4) and paleosol (MIS 3)

Unit 8 is a thin, 0.25 – 1.25 m, discontinuous, oxidized silt with some sand, crude horizontal bedding, and mottles. This unit is laterally discontinuous and found only in 3 sections at Granite Creek. It has approximately 15% pebbles incorporated in the top 0.75 m. At location GRC-01W, the lower contact is sharp, and is draped over Unit 5, potentially a buried MIS 4 alpine moraine. Oxidation and mottling within the loess is gradational and extends into the underlying morainal sediment. This unit is interpreted as MIS 4 deglacial loess with a MIS 3 paleosol imprinted onto the former surface.

Strat log:

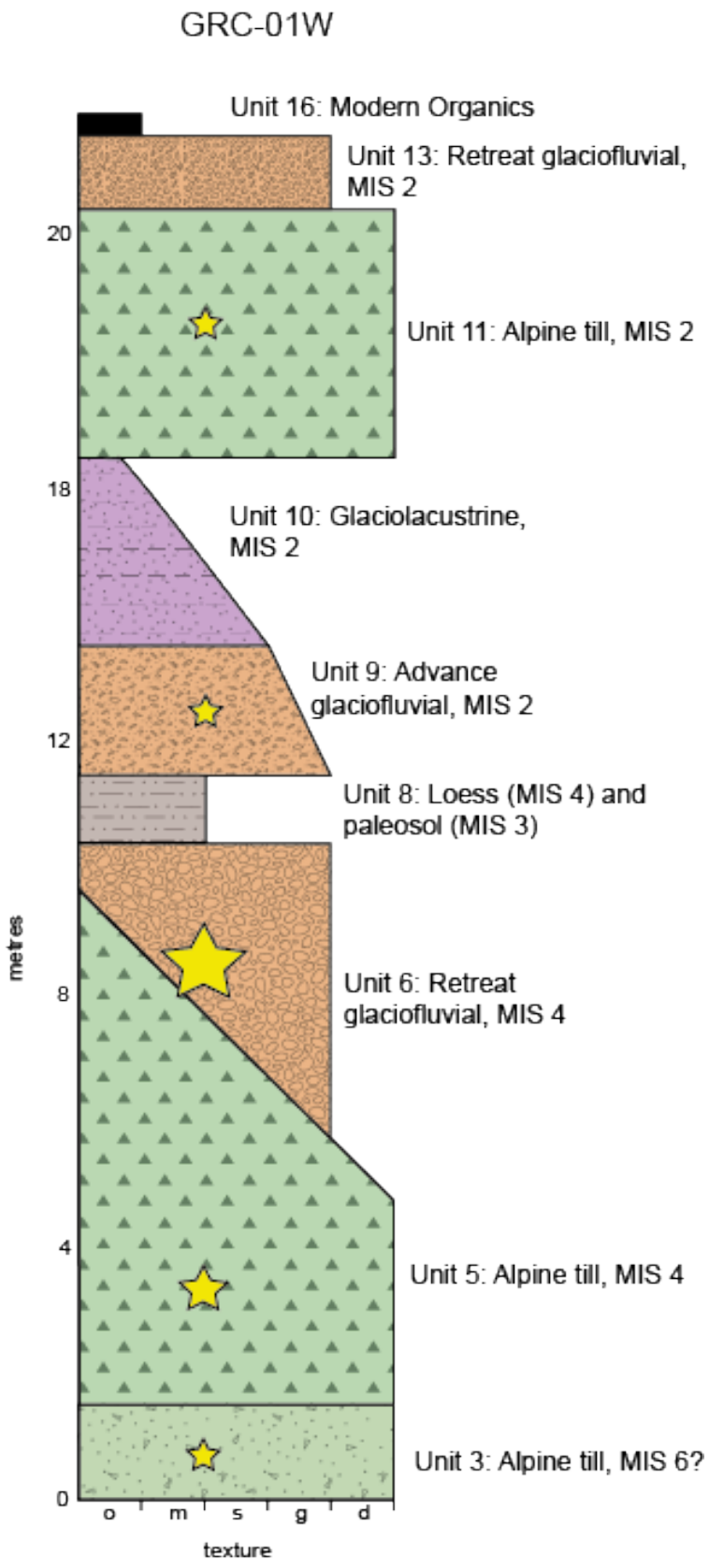
GRC-01W
Unit 16: Modern Organics
Unit 13: Retreat glaciofluvial, MIS 2
Unit 11: Alpine till, MIS 2
Unit 10: Glaciolacustrine, MIS 2
Unit 9: Advance glaciofluvial, MIS 2
Unit 8: Loess (MIS 4) and paleosol (MIS 3)
Unit 6: Retreat glaciofluvial, MIS 4
Unit 5: Alpine till, MIS 4
Unit 3: Alpine till, MIS 6?
metres
20
18
12
8
4
0
o
m
s
g
d
texture

Photos:

Figure 11: Sample location for 21JS-022

Figure 12: Sample location for 21JS-023

Figure 13: Upper contact of Unit 8.

Figure 14: Bottom contact of Unit 8.

Figure 15: Unit 8 is beside tape measure, and Unit 5 is below (bouldery morainal unit).

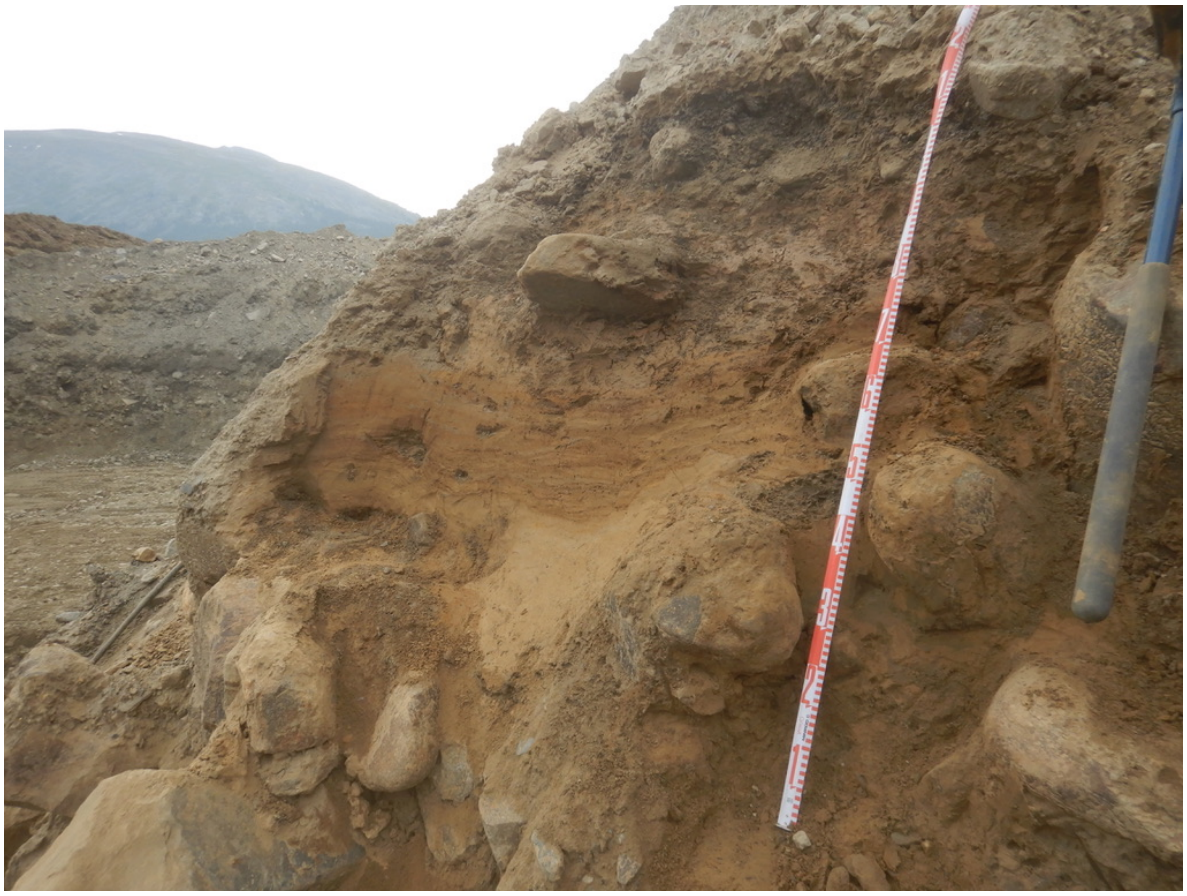

Figure 16: Unit 8 and upper contact (gradational) and lower contacts (sharp).

Sample:

21-JS-051

21JS-052 (Moisture)

Unit description: Originally inferred to be Unit 8 loess (MIS 4) and paleosol (MIS 3) in YGS paper and strat log below, however there is a lack of preserved till in this section and therefore it is difficult to correlate. It is likely that this unit is Holocene loess.

Description:

Thickness: 0.2 – 0.5 m

Texture: 90% brown/oxidized clayey silt with 10% rounded-subrounded, oxidized and pitted pebbles

Colour: Reddish brown

Structures: None

Organics: Roots/root casts (sampled)

Contacts: lower – draped over coarse outwash gravel. Upper – becomes more clast rich with pebbles towards top. The upper contact is sharp with poorly sorted gravel.

Interpretation: Loess and paleosol

Strat Log:

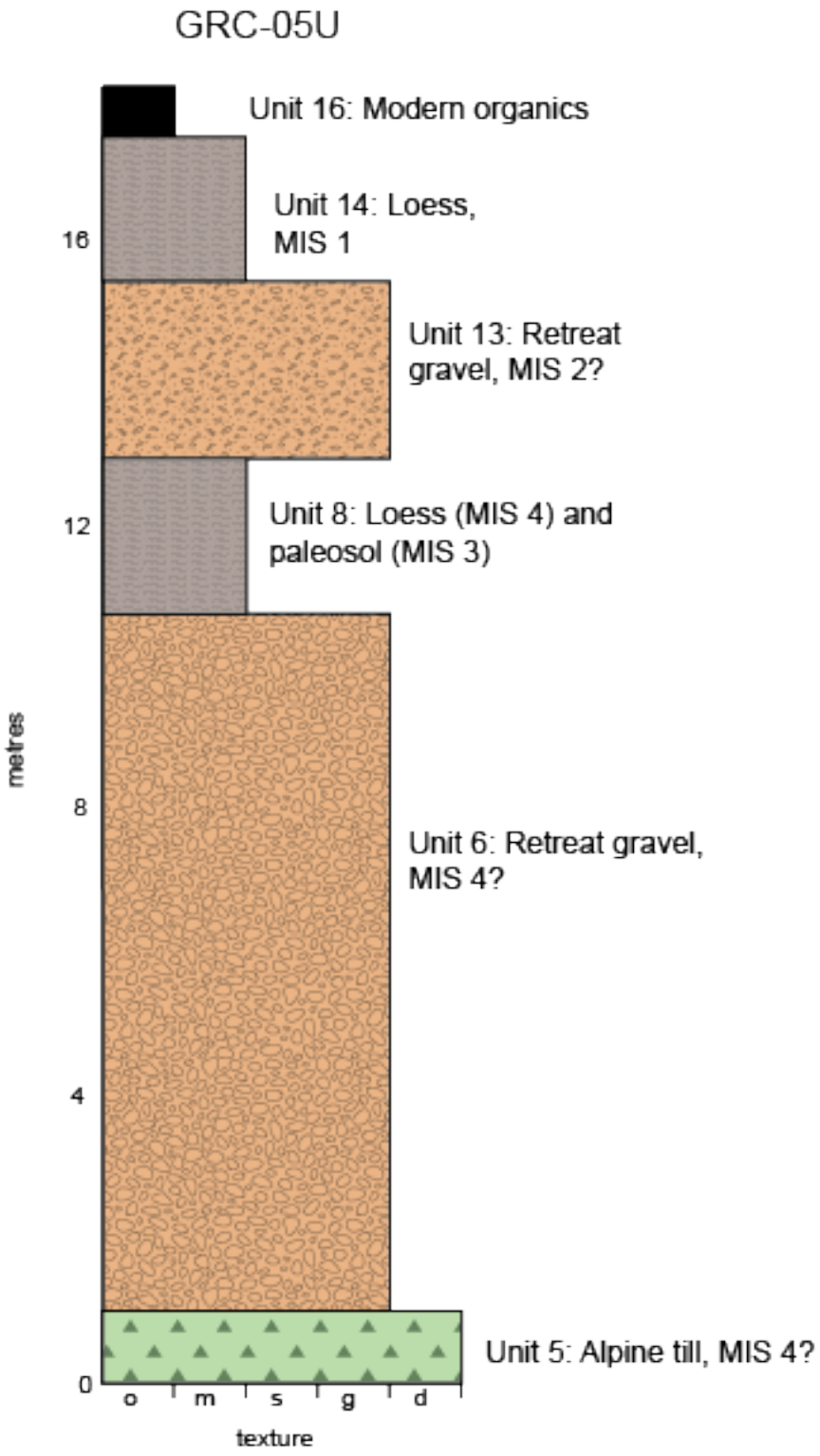
GRC-05U
Unit 16: Modern organics
Unit 14: Loess, MIS 1
Unit 13: Retreat gravel, MIS 2?
Unit 8: Loess (MIS 4) and paleosol (MIS 3)
Unit 6: Retreat gravel, MIS 4?
Unit 5: Alpine till, MIS 4?
metres
16
12
8
4
0
o
m
s
g
d
texture

Photos:

Figure 17: Unit 8 with upper and lower gravel.

Figure 18: Around the corner from the location where we sampled.

Figure 19: Unit 8 on sample day.

Figure 20: 21JS-051 OSL Sample location.

Sample:

21JS-061

21JS-062 (Moisture)

Unit description:

Note that for the YEG YGS paper, I grouped this unit into Unit 3: Alpine till, MIS 6. I did not describe the black sand section in this paper because it seems to pertain more to glacial history than to placer forming environments as it is a small part of a complicated unit and I did not want to overcomplicate the description.

Description of black sand portion:

Thickness: 1.4 m, length is 3.4 m

Texture: 90% medium sand, 10% fine sand and 5% clasts (pebbles)

Colour: 2.5Y3/0 (dark gray)

Structures: Deformed silt beds. Inclusions of very fine-grained beige sand

Organics: None

Contacts: Lower – seems to be same material as gravelley till to the west

Top is overridden by Unit 5 alpine till, MIS 4

Interpretation: glaciofluvial sand, glaciotectonized and incorporated into till

Rest of the unit:

Unit 3 is a discontinuous, silty, overconsolidated olive brown to beige diamict with abundant rounded to subrounded clasts. This unit found only in GRC-01W, is discontinuous and has a thickness of 0 – 3 m. Clast content is highly variable and averages 35%, with 20% pebbles, 75% cobbles and 5% boulders. The matrix is medium sand with some thin silt beds found under boulders. Clasts are subrounded to rounded. Lithologies are dominantly quartzite, but 10 highly weathered granitic pebbles and cobbles were found in section GRC-01W. The lower contact was not exposed. This unit contains low amounts of gold.

This unit is interpreted as being till due the presence of erratics and clast fabric indicating flow out of the Granite Creek cirque. The presence of weathered granitic erratics suggests that this unit reworked sediments deposited by the retreat of the CIS during an older glaciation. Granite bedrock is not present in upper Granite Creek basin and originates from the Roop Lakes Pluton, approximately 20 km to the east. The age is interpreted as MIS 6 due to its stratigraphic position underlying inferred MIS 4 till at location GRC-01, however it is possible that this deposit is from an older glaciation or an earlier phase of the MIS 4 advance.

Strat Log:

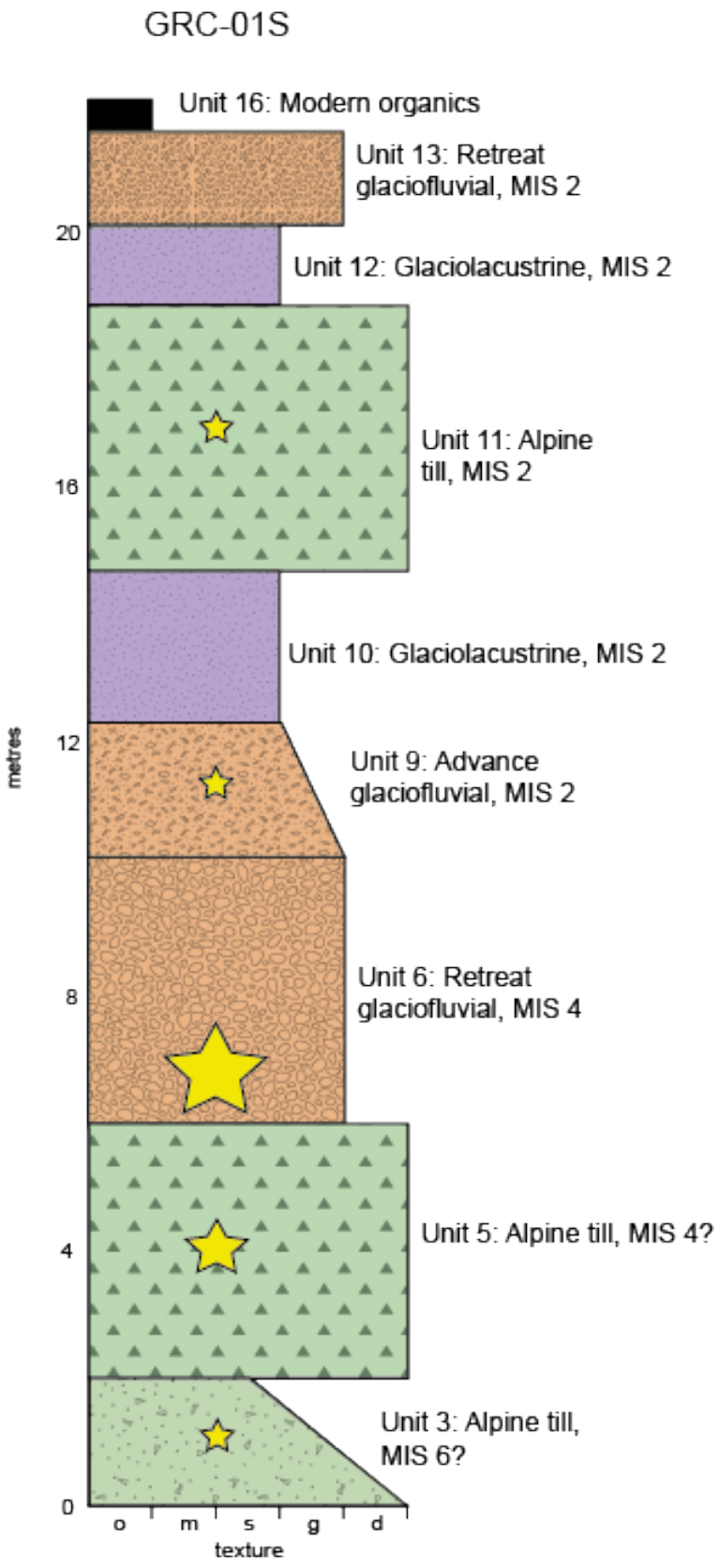
GRC-01S
Unit 16: Modern organics
Unit 13: Retreat glaciofluvial, MIS 2
Unit 12: Glaciolacustrine, MIS 2
Unit 11: Alpine till, MIS 2
Unit 10: Glaciolacustrine, MIS 2
Unit 9: Advance glaciofluvial, MIS 2
Unit 6: Retreat glaciofluvial, MIS 4
Unit 5: Alpine till, MIS 4?
Unit 3: Alpine till, MIS 6?
metres
20
16
12
8
4
0
o
m
s
g
d
texture

Photos:

Figure 21: Black sand grouped into Unit 3 alpine till, MIS 6. Sharp contact with Unit 5 alpine till, MIS 4 above.

Figure 22: 21JS-061 OSL Sample location.

Figure 23: Black sand grades into gravelley till to the west.